Geometrical characterization of liquid core fibers by measurement of thermally induced mode cutoffs and interference

Susana A. Planas, Erik Bochove, and Ramakant Srivastava

Transmitted and scattered intensity in liquid core fibers have been measured as a function of temperature and v values of cutoff points obtained which are in good agreement with weakly guiding mode theory. We also report observation of oscillations in the transmitted intensity which we interpret to be caused by interference between modes. We show that measurement of the period of these oscillations can be used to make high-precision nondestructive measurements of core radius and core ellipticity along the fiber length.

I. Introduction

Liquid core fibers (LCF), although not serious candidates for optical communications, offer a suitable medium to study propagation properties of step-index fibers: in the early 1970s work[1] on multimode LCFs included selective launching and measurements of attenuation and dispersion. Recently, their polarization properties have also been studied[2] because of the attractive possibility of their application as current sensors. On the other hand, many techniques have been developed for the characterization of solid core fibers in the near single-mode region,[3] and recently interest has developed in polarization-maintaining single-mode fibers[4] where strain or ellipticity cause high birefringence. Temperature dependence of birefringence in single-mode[4] and multimode[5] fibers has also been studied, but little work on LCFs exists.

In this work we exploit the high value of the temperature dependence of the refractive index of liquids as a fiber core material to make novel studies of guiding properties of LCFs. Varying the temperature of a short fiber segment and thereby attaining large variations in the v value, mode cutoffs were observed in transmitted as well as scattered radiation, and the cutoff v values were compared with those predicted by weakly guiding mode theory.[6] Besides the cutoffs we observe periodic variations in transmitted intensity as a function of v value. The oscillations were enhanced by introduction of a pinhole in front of the detector, thereby causing truncation of the field pattern incident on the detector.

We interpret these oscillations as due to interference between guided modes, a hypothesis which was found to be supported by the simple interference theory of two and three sinusoidal signals. Moreover, we identified the presence of two different periodicities in the transmitted intensity which differed by an order of magnitude. We show that the oscillations with smaller period are caused by interference between different LP mode groups. We used this assumption to calculate the core radius with high precision, yielding thereby a value in good agreement with that obtained by the cutoff measurements.

The oscillations of larger period we have interpreted as being due to birefringence caused by core ellipticity. The values of the period predicted by theory support this interpretation and provide a nondestructive method to measure accurately core ellipticity.

In both the core radius and ellipticity determinations the measurements can be performed on several LP mode groups, thereby offering a means of comparison and a consistency check.

II. Experimental

Hollow quartz fibers of a few meters in length, 10–12-μm internal diameter and ~80-μm of external diameter were filled with liquids (light and heavy paraffin oil) using the hydrostatic filling process.[7] The characteristics of the fibers used are given in Table I. The

When this work was done all authors were with Universidade Estadual de Campinas, Instituto de Fisica, Campinas, 13.100-SP, Brazil; Erik Bochove is now with Centro de Pesquisa e Desenvolvimento-CPqD, Telebras, Campinas, 13.100-SP, Brazil.

Received 12 November 1981.
0003-6935/82/152708-08$01.00/0.

Table I. Characteristics of the Fibers Used

Fiber	Radius (μm)	Liquid
C,D,E,F	5.5	Light paraffin
A	6.0	Heavy paraffin
B	5.8	Light paraffin

Table II. Refractive Index Data for the Fibers Used

	n (5890 Å)	T (°C)	n (6328 Å)	dn/dT (°C^{-1})
Light paraffin	1.4644	21.1	1.4620	
	1.4626	25.9	1.4602	-3.6×10^{-4}
	1.4594	35.0	1.4570	
Heavy paraffin	1.4680	29.4	1.4656	
	1.4620	46.0	1.4595	-3.7×10^{-4}
	1.4585	55.5	1.4561	
Quartz	1.4585	—	1.4571	-3×10^{-6}

refractive index of the liquids at 5890 Å was measured from 10 to 60°C with an Abbe refractometer, and assuming linear dispersion, these values were corrected to calculate the refractive index at the wavelength of the radiation used in the present work ($\lambda = 6328$ Å). Table II gives some of the refractive-index values at different temperatures for the liquids and the cladding material (quartz). As expected, the refracted index varies linearly with temperature.

The experimental arrangement for measurement of transmitted intensity is shown in Fig. 1. The fiber was maintained straight all along its length, and the part before the furnace was supported in a V-groove containing a black oil. This removes the cladding radiation and also functions to prevent movement of the fiber and assist in maintaining a uniform temperature. Maintaining the fiber steady is essential to limit modal noise. Both ends of the fiber were immersed in cells containing the same paraffin as the core.

Approximately 20 cm of fiber length were maintained in an oven made of two concentric cylinders. The fiber passes through the inner copper cylinder containing a dark oil to remove quickly any cladding radiation due to temperature-induced mode cutoffs. A thermocouple immersed in this liquid measures the temperature. In the space between the two cylinders water of controlled temperature was circulated. The heating rate, below 0.5°C/min, was sufficiently slow that the system could be maintained in quasi-thermal equilibrium.

About 1 mW of power from a He–Ne laser was coupled into the fiber by a 10× microscope objective. Since at room temperature our LCFs supported many modes, for efficient selective launching of desired modes the fiber was maintained at a temperature corresponding to a v value just above the cutoff point of the desired mode. At this point the launching conditions were adjusted using angular and translational movements of the fiber end until the power coupled reached a maximum. Convenient identification of the mode or combination of modes coupled was made by inserting a polarizer and analyzer in the light path.[8]

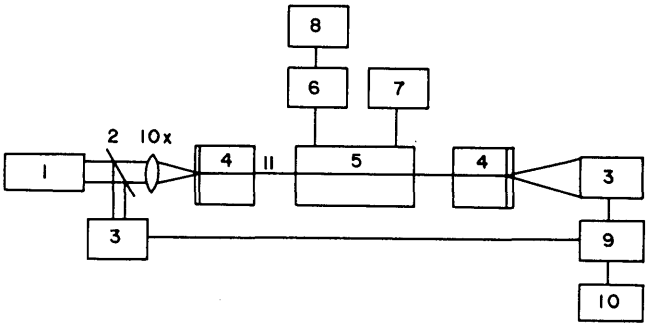

Fig. 1. Block diagram of the experimental arrangement: 1, He–Ne laser; 2, beam splitter; 3, power meter; 4, liquid cell; 5, furnace; 6, thermocouple; 7, temperature controller; 8, digital voltmeter; 9, voltage divider; 10, chart recorder; and 11, fiber.

The intensity of the transmitted light was detected by a photodetector placed at the output end of the fiber and corrected for possible laser fluctuation by using a ratiometer. Measurements of the scattered signal were made using a lock-in amplifier. In this case the segment of the fiber between the furnace and the liquid cell was placed between two large area photodetectors using an index-matching liquid. The data were recorded on a chart recorder. It must be pointed out that the temperature variation was not linear in time but was sufficiently linear to allow measurements of the periods of oscillations with great precision.

III. Results

Figures 2–4 show temperature dependence of transmitted intensity by three fibers: *D*, *A*, and *B*. The abscissa is linear in time but only approximately linear in temperature. The corresponding v values were calculated by inserting a, λ, and n in Eq. (4) in Ref. 6 and using the n_c vs T curve. As the temperature increases Fig. 2 shows flat regions where the intensity is almost constant. As mode cutoff is approached leakage of power from core to cladding occurs, and the transmitted intensity decays; however, it has been found that the mode cutoff is not abrupt but somewhat gradual. We assign the value of v at cutoff v_c as the point where no transmitted intensity is detected in the respective mode.[9]

The identification of the v_c values was also simultaneously confirmed by two methods: (1) observing the near-field mode pattern with the help of analyzers, as described in Ref. 8; and (2) measuring the positions of the peaks in the scattered intensity as described by Midwinter and Reeve.[9] The vertical arrows indicate the location of the theoretical and experimental v_c values. With these criteria the experimental v_c values are in good agreement with those predicted by the weakly guiding mode theory.[6]

Theoretically, the LP_{01} mode has cut off only at the temperature where the refractive index of the liquid equals that of the cladding material. However, in practice, very little light reaches the detector near temperatures corresponding to $v_c \approx 1.0$, where for practical purposes the field is no longer guided.[6] As can

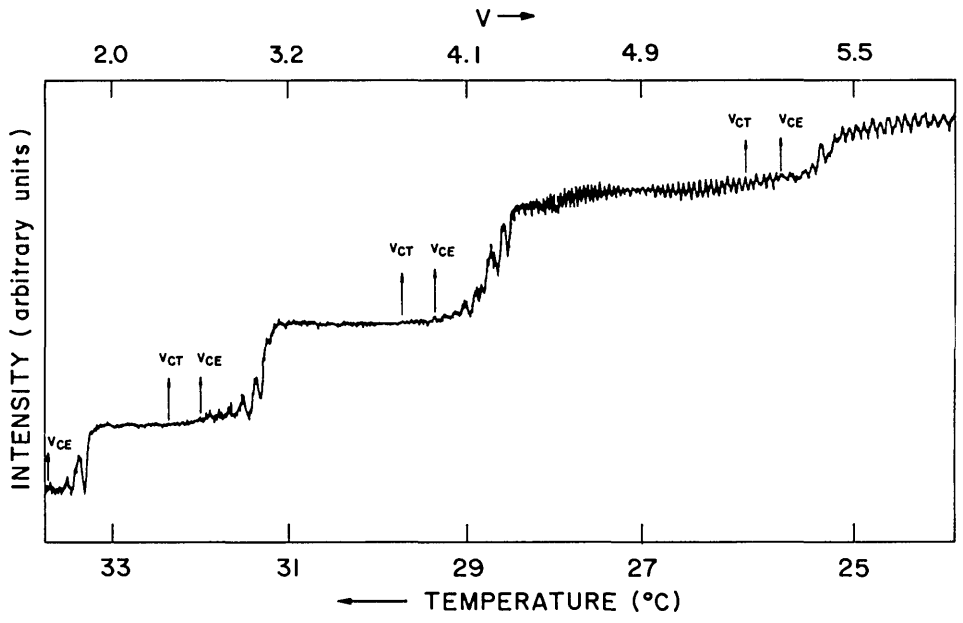

Fig. 2. Transmitted intensity of fiber D as a function of temperature and v value. v_{CE} and v_{CT} are the experimental and theoretical mode cutoff v values respectively.

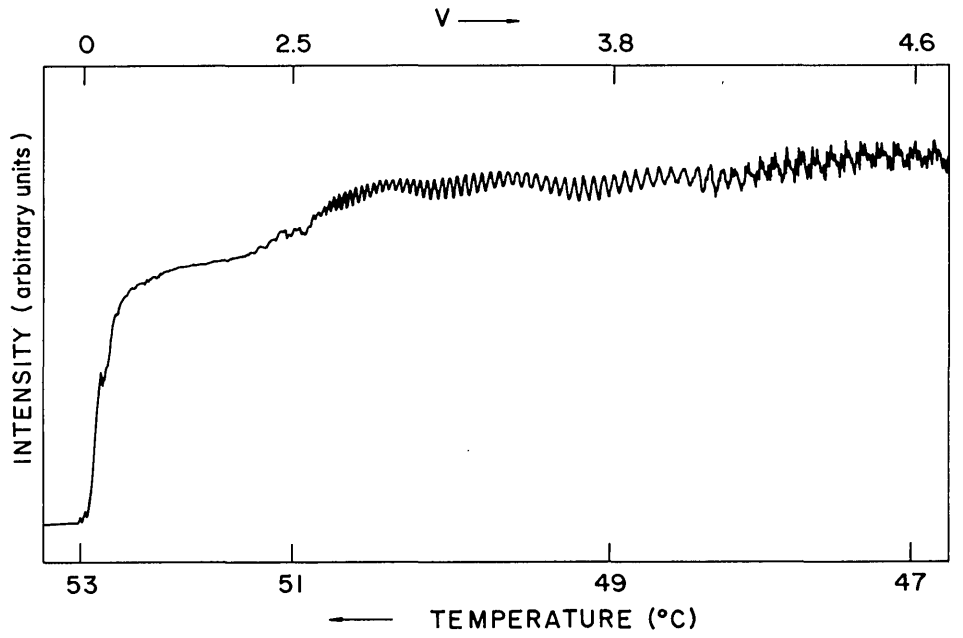

Fig. 3. Transmitted intensity as a function of temperature and v value for fiber A.

be seen from Fig. 2, the theoretical v_c values v_{CT} are always lower than the corresponding experimental values v_{CE}.

The sharp spikes near the cutoff region are present whenever the removal of cladding radiation in the furnace is incomplete. When a conventional air furnace was used with no mechanism to remove cladding radiation within the furnace, these spikes were abundant in the data, causing difficulty in identification of cutoff points and measurement of oscillation periods. However, when the fiber was placed in the liquid oven, these variations almost disappeared, indicating that they were caused by cladding radiation.

Another distinct feature in Fig. 2, besides the cutoffs, is the presence of periodic oscillations in the intensity below 29°C. In the region between 25 and 29°C we identify two kinds of oscillations, one of period ~0.05°C, and the other is observed as slow modulation of the former with a period an order of magnitude higher. By visual observation of the near-field pattern and the fact that the oscillations disappear at cutoff we identify one of the interfering modes as the LP_{02} mode group. The other interfering mode group is expected to be either the LP_{11} or LP_{01}. As is shown in Sec. V, only the interference between LP_{11} and LP_{02} mode groups can explain our observed data.

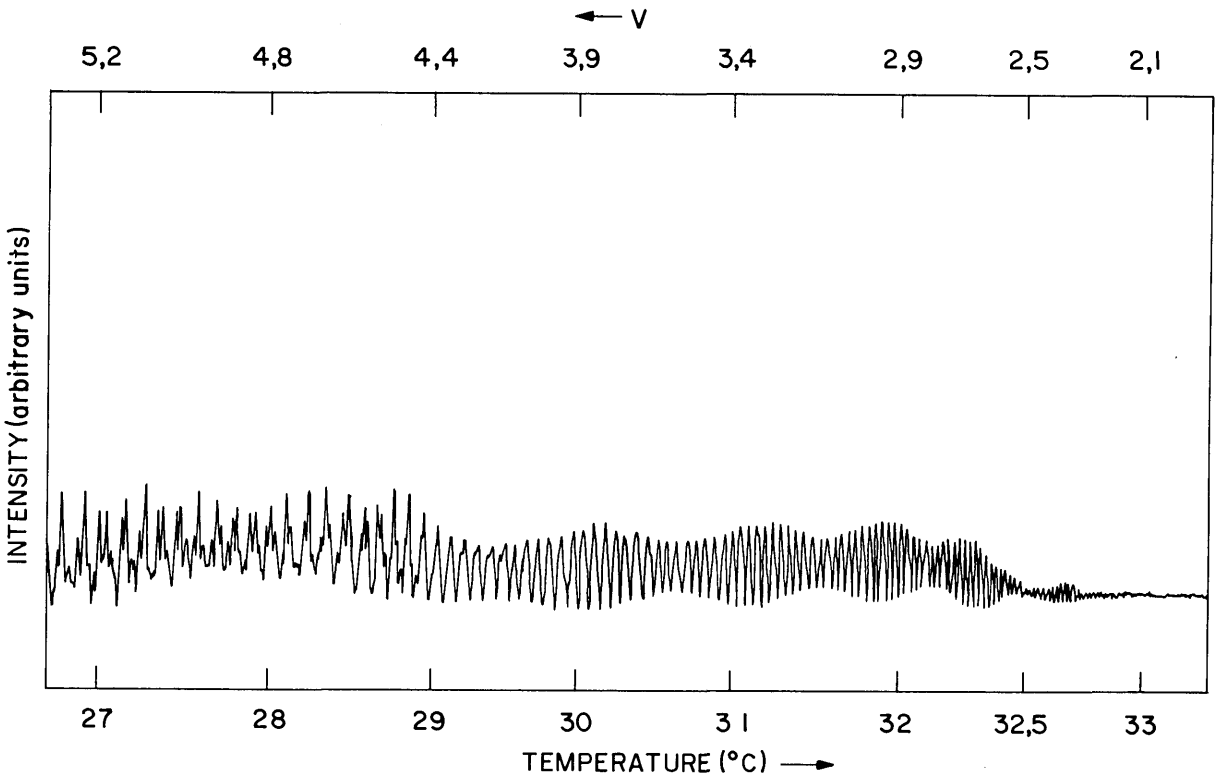

Fig. 4. Transmitted intensity of fiber B as a function of temperature and v value with a pinhole in front of the detector.

The slow modulation is explained by the interference of three modes within the LP_{11} and LP_{02} groups. We did not verify this hypothesis in this case but verified its validity for interference between LP_{01} and LP_{11} mode groups in the $v = 3$ to $v = 4$ region in other fibers, as discussed below.

Figure 3 shows the variations in the transmitted intensity when the fiber A was heated. The mode cutoffs in this case are not marked by any appreciable drop in intensity because very little energy was coupled into the higher-order modes. Experimentally these points can be identified by noting that the oscillation pattern does show a sudden change when a mode ceases to be propagated. Between 47 and 48°C the oscillations have a complex structure reminiscent of interference between three or more LP modes. Using the criterion mentioned in the description of Fig. 2 we have identified the interfering modes in this region as being LP_{01}, LP_{11}, and LP_{21}. This structure becomes simpler below the cutoff point of LP_{02}–LP_{21} modes at ~48°C. The oscillations disappear at the LP_{11} mode cutoff at ~51°C where only the fundamental LP_{01} mode is guided.

Referring back to Fig. 2, we notice the absence of oscillations in the region below $v = 4$. As will be seen later in Sec. IV, this is because all the light in the interfering modes falls on the detector. However, the amplitude of interference between modes may be enhanced by truncating the field pattern of the modes involved on the detector surface by placing a pinhole or other spatial filter in front of the detector, thus helping in the precise measurement of the period of oscillations. On the other hand, this may complicate the interference of higher-order modes. Figure 4 shows such an enhancement in fiber B. We can clearly see that below 29°C almost all the guided modes interfered, causing a complex structure in the transmitted intensity pattern. As the temperature increases mode cutoffs occur, and the structure becomes simpler until ~33°C when only the fundamental LP_{01} mode propagates.

In the succeeding sections we show that our results can be explained by relatively simple theory.

IV. Theory

A. Basic Equations of Beat Phenomena

Assuming that no mode coupling occurs, the total power measured by a detector which is placed at a small distance from the output end of the fiber is given by the sum over the powers contributed by individual modes plus a contribution from interference between mode pairs:

$$P_d = \sum_n p_n f_n \exp[-\alpha_n(T)L] + \sum_{m \neq n} \sqrt{p_n p_m}\, f_{nm} \exp[-\tfrac{1}{2}[\alpha_n(T) + \alpha_m(T)]L] \cos\{[\beta_n(T) - \beta_m(T)]L + \phi_n - \phi_m\}, \quad (1)$$

where p_n = output power in the nth fiber mode omitting loss in the furnace;
α_n = temperature-dependent power-loss coefficient of nth mode inside furnace;
L = length of fiber inside the furnace;
f_n = fraction of light in the nth mode which is detected;
f_{nm} = mode overlap integral at the detecting surface, given in Eq. (2) below;
β_n = temperature-dependent propagation constant of the nth mode inside the furnace; and
ϕ_n = constant phase term.

The interference is controlled by the functions f_{nm} given by

$$f_{nm} = \frac{\int d\mathbf{e}'_n(\rho) \cdot \mathbf{e}'_m(\rho) d^2\rho}{[\int \mathbf{e}_n^2(\rho) d^2\rho]^{1/2} [\int \mathbf{e}_m^2(\rho) d^2\rho]^{1/2}}, \quad (2)$$

where the integral in the numerator is performed over that part of the detector surface which is exposed to the light, and the integrals in the denominator are over the entire plane of the detector surface. The fields $e'_n(\rho)$ are related by a diffraction integral to the fiber mode fields $\mathbf{e}_n(\rho)$. To observe interference it is necessary that $f_{nm} \neq 0$ for at least one mode pair. It may be shown[10] that the fields $e'_n(\rho)$ are very nearly orthogonal for free-space propagation between the fiber end and the detector surface (the small discrepancy being due to evanescent fields which decay in the direction of the axis). It is therefore necessary to enhance the interference by truncating the field over the detector surface by employing a pinhole.

Equation (1) describes all temperature dependence of losses and interference through the temperature dependence of α_n and β_n, respectively. To describe the mode cutoff effect as a function of temperature, no more detailed theoretical analysis is needed, except the observation that the cutoff of the nth mode is defined as the point where $\exp(-\alpha_n L)$ vanishes. On the other hand, to explain the mode interference we must use exact expressions for the relevant $\beta_n(T)$. These functions depend on the modal properties of the fiber as well as the temperature dependence of the refractive index of the liquid core. Measurements of the interference pattern of a relatively small number of modes (two or three) would, in principle, allow for a means of studying propagation properties of fiber lengths equal to that of the furnace.

In those cases in which the variation in oscillation period over several periods of an observed interference pattern is small compared with the period itself, it is useful to consider $\beta_n(T)$ as the linear function of T in the neighborhood of a reference point. This is done below for the cases of two and three-mode interference, respectively.

1. *Interference of Two Modes*

Lumping terms which are irrelevant to the present discussion, Eq. (1) simplifies to

$$P_d^{(2)} = C_0 + C_{12} \cos[(\beta_1 - \beta_2)L + \phi_1 - \phi_2], \quad (3)$$

showing explicitly only the interference term. Considering the temperature as variable, the frequency of oscillations is defined by

$$\nu_{12}(T) = \left(\frac{1}{2\pi}\right) \cdot \frac{d}{dT}(\beta_1 - \beta_2)L \quad (4)$$

in the manner discussed above. An expression for $\nu_{12}(T)$ in the case of interference between two LP mode groups of the circular fiber will be derived in Sec. IV.B.

2. *Interference of Three Modes*

For the case of three modes, considering again explicitly only the interference terms, Eq. (1) has the form

$$\begin{aligned} P_d^{(3)} = C_0 &+ C_{12} \cos[(\beta_1 - \beta_2)L + \phi_1 - \phi_2] \\ &+ C_{23} \cos[(\beta_2 - \beta_3)L + \phi_2 - \phi_3] \\ &+ C_{13} \cos[(\beta_1 - \beta_3)L + \phi_1 - \phi_3]. \end{aligned} \quad (5)$$

This rather complicated equation fortunately simplifies to a form which is consistent with our data, if certain relations among the constants C_{nm} and β_n are assumed. Thus take $\beta_1 \cong \beta_2$ and $C_{13} = C_{23}$. The first condition is satisfied when modes one and two belong to the same LP mode group. The second condition requires equality of powers and overlap fractions: $p_1 = p_2$ and $f_{13} = f_{23}$, which is also likely to be met when the modes one and two belong to the same LP group. Equation (5) becomes

$$\begin{aligned} P_d^{(3)} \cong C_0 &+ C_{12} \cos[(\beta_1 - \beta_2)L + \phi_1 - \phi_2] \\ &+ 2C_{13} \cos[\tfrac{1}{2}(\beta_1 - \beta_2)L + \tfrac{1}{2}(\phi_1 - \phi_2)] \\ &\times \cos[(\beta_3 - \beta_1)L - \tfrac{1}{2}(\phi_1 + \phi_2) + \phi_3]. \end{aligned} \quad (6)$$

The third term in this equation is the most important for our purposes. It oscillates at the frequency

$$\nu_{13}(T) = \frac{1}{2\pi} \frac{d}{dT}(\beta_3 - \beta_1)L, \quad (7)$$

while its amplitude is modulated at the lower frequency $\nu'_{12}(T) \ll \nu_{13}(T)$:

$$\nu'_{12}(T) = \frac{1}{4\pi} \frac{d}{dT}(\beta_1 - \beta_2)L. \quad (8)$$

The second term in Eq. (6) results in a bending of the pattern described by the remaining terms. This effect is not observed in the data of Fig. 2, although it can be seen in Fig. 3. The reason must be found in the assumption that in the former case the intensity in modes one and two is small compared with mode three, as C_{13} is proportional to $\sqrt{p_1 p_3}$, yielding $C_{12} \ll C_{13}$.

In Secs. IV.B and C, explicit expressions for the beat periods of three interfering modes will be derived in terms of fiber mode parameters. It is assumed that the smaller period is due to interference between two different LP mode groups and the larger due to birefringence induced by core ellipticity.

B. Beating Between LP Mode Groups

We express the propagation constant of a given LP mode in terms of the parameter b of weakly guiding mode theory,[6] the wave number k, cladding index n, and refractive-index difference $\Delta = (n_c - n)/n$, where n_c is the core index and

$$\beta = nk(1 + b\Delta). \tag{9}$$

Differentiating this equation with respect to temperature T yields

$$\frac{d\beta}{dT} = nk\left(b + \tfrac{1}{2}v\frac{\partial b}{\partial v}\right)\frac{d\Delta}{dT}, \tag{10}$$

where

$$v = nka\sqrt{2\Delta} \tag{11}$$

is the normalized frequency. The derivative $\partial b/\partial v$ may be eliminated by means of Eq. (25) of Ref. 6:

$$\frac{\partial}{\partial v}(bv) = b + 2\kappa(1 - b), \tag{12}$$

where $\kappa = K_l^2(w)/K_{l+1}(w)K_{l-1}(w)$ and $w = \sqrt{b}\,v$. Using the expression[6]

$$R = 1 - (u^2/v^2)(1 - \kappa), \tag{13}$$

where $u = v\sqrt{1-b}$, for the ratio of power guided by the core to total power, Eq. (10) becomes

$$\frac{d\beta}{dT} = k\frac{dn_c}{dT}R. \tag{14}$$

By Eq. (4) the period of the beats between two different LP modes having the values R_1 and R_2, respectively, for the fraction R is given by

$$P_{12} = \frac{2\pi}{kL\dfrac{dn_c}{dT}|R_1 - R_2|}. \tag{15}$$

We also derived this result from coupled-mode theory.[11]

C. Beating Induced by Core Ellipticity

A small ellipticity of the core induces birefringence of the fundamental mode of the fiber in the manner that the difference in propagation constant between x and y polarizations is given by Snyder and Young[12]:

$$\beta_x - \beta_y = \frac{e^2(2\Delta)^{3/2}}{8a}\frac{u^2w^2}{v^3}\left[1 + u\frac{K_0^2(w)}{K_1^2(w)}\frac{J_2(u)}{J_1(u)}\right], \tag{16}$$

where

$$e = \text{core eccentricity} = [1 - (\text{minor axis/major axis})^2]^{1/2}. \tag{17}$$

Likewise, for higher-order modes ($l \geq 1$), a beating is observed between modes which are a combination of the linearly polarized modes possessing, respectively, even and odd symmetry under 90° rotation and under reflections in the x and y axes.[12] For the particular case $l = 1$,

$$\beta_e - \beta_o = \frac{e^2}{4a}\sqrt{2\Delta}\frac{u^2}{v}\kappa. \tag{18}$$

For the small eccentricity observed in our fibers the beat period predicted by Eqs. (16) and (18) is much greater than that of interference between different LP groups discussed above. Where both effects take place Eqs. (7) and (8) may thus be applied to give the beat periods for interference between LP groups and birefringence, respectively. The calculation of the latter yielded a rather complicated result so we shall omit it here.

V. Discussion

A. Mode Cutoffs

As mentioned earlier we used three simultaneous observations to identify cutoff points for the modes; the sudden change in the transmitted intensity level, change in the modal pattern in the near field, and the positions of the peaks in the scattered radiation as a function of temperature. We find that the cutoff values obtained by measuring the positions of the peaks in the scattered radiation are coincident with those obtained by the criterion used in the transmitted intensity. It must, however, be added that due to microbendings present in the fiber, it is not always possible to locate the peak positions accurately because of the structure present in each peak near the corresponding cutoff point. We find, therefore, that it is more accurate to assign the cutoff in the transmitted intensity curve. Using any of the three criteria mentioned above, we have reproduced the values of cutoff temperatures with an accuracy of better than 0.1°C.

In all measurements we have found that the theoretical v values of cutoffs lie lower than the corresponding experimental values. This is well-understood and has been observed in single-mode glass fibers using different techniques to measure the cutoff wavelength of the LP_{11} mode.[13] The cause has been assigned to the presence of bending, cladding imperfections, microbendings, and other forms of fiber irregularity such as boundary variations. The fact that the cutoff is gradual and not abrupt even in a liquid core fiber is also related to the factors mentioned above. In our experiments we tried to keep the fiber straight all along its length in an attempt to minimize the bending effects and have been able to obtain a close agreement between v_{CE} and v_{CT}.

The experimental cutoff temperatures indicated by arrows in Fig. 2 can be used to calculate the core radius if we assume that they correspond to the theoretical cutoff v values given by the weakly guiding mode theory. The maximum error caused by this assumption is 8%. But the value of the radius calculated using all the cutoff points can be averaged to improve the accuracy. We will demonstrate below that the measurement of oscillation periods provides a method to determine the core radius with even higher accuracy.

B. Oscillations

The experimental results show two types of oscillations, one with period τ_1 ranging between 0.02 and 0.08°C, and another as beats of period τ_2 ranging between 0.3° and 1.3°C. Below we discuss how these oscillations can be explained on the basis of interference

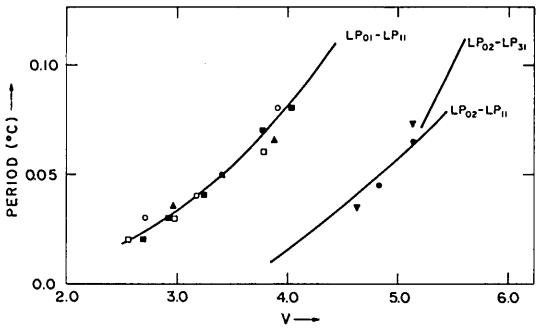

Fig. 5. v dependence of the period due to interference between pairs of LP mode groups. The solid line represents theoretical values, and the points refer to various fibers: ▲, fiber A; ○, fiber B; ■, fiber C; □, fiber F; ▼, fiber D; ●, fiber E.

between LP mode groups and birefringence induced by core ellipticity.

1. *Interference Between LP Mode Groups*

As mentioned in Sec. III by visual observation of the near-field pattern it was not always possible to identify completely the set of modes which cause oscillations, particularly in the case of interference between higher-order modes. In most cases, however, it was possible to identify visually at least one of the interfering mode groups without any ambiguity. The other one was then identified by comparison with theory in the following way:

The experimental values of τ_1 as a function of v were determined for various fibers. Figure 5 shows our data for some of the fibers measured. The solid curves in the same figure represent the theoretical values of the interference periods for pairs of LP mode groups obtained by using Eq. (15). The values of the parameters R_1 and R_2 were obtained from the weakly guiding mode theory given by Gloge.[6] The close agreement between the theoretical and experimental values seen here can, therefore, be used to identify which pairs of mode groups are involved in each interference pattern. Moreover, the best fit of the theoretical curve to the experimental data can be obtained by using the core radius as an adjustable parameter. We have found that the value of the core radius determined by this fit is very close to that obtained using an optical miscroscope or from the values of v_{CE} of various modes for the corresponding fiber. In fact, we find that this technique for determining the core radius of a hollow fiber is much more precise than optical microscopy. From our data we estimate that we can measure the core radius to a precision of better than 5%. This corresponds to a precision of 0.3 μm in a typical case. However, in the case of fiber C we have obtained a precision of 0.1 μm in measurement of core radius.

2. *Interference Caused by Core-Ellipticity Induced Birefringence*

Considering again the oscillations shown in Figs. 2, 3, and 4, it is seen that a slow modulation of period ranging between 0.3 and 1.3°C appears in the region of

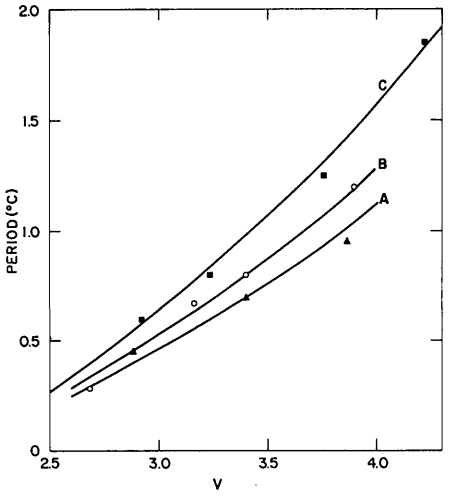

Fig. 6. v dependence of the period due to ellipticity induced interference between ${}_oLP_{11}$ and ${}_eLP_{11}$ modes. The solid curves represent the theoretical values corresponding to experimental data for fibers A, B, and C.

$2.4 < v < 3.8$. On the other hand, no oscillation is observed in the region of single-mode propagation ($v < 2.4$).

In the presence of a small amount of core ellipticity, one would expect to see beats between the ${}_xLP_{01}$ and ${}_yLP_{01}$ modes. Furthermore, the modulation of the beat pattern between 2.4 and 3.8 v values should be caused by interference between ${}_xLP_{01}$, ${}_yLP_{01}$, ${}_oLP_{11}$, and ${}_eLP_{11}$ modes.

Using Eqs. (16) and (18) it is now easily explainable why the beating of the fundamental LP_{01} mode is not observed. The former equation shows a dependence of the birefringence proportional to $(2\Delta)^{+3/2}$ and the latter proportional to $(2\Delta)^{+1/2}$. As other terms are of approximately the same magnitude and with $\Delta < 0.01$, this means that the birefringence due to core ellipticity in the fundamental mode is <1% that of the LP_{11} mode group. The period of oscillation predicted is thus much greater than the temperature interval over which the fiber is single mode.

Considering now the interference of LP_{11} and LP_{01} mode groups, the birefringence of the latter is neglected with respect to the former by the same argument as above. Consequently we are justified in applying the three-mode interference theory of Sec. IV.B. Using Eq. (18) for the difference ${}_e\beta_{11} - {}_o\beta_{11}$ and applying Eq. (8) for the period of slow modulation, a theoretical expression is obtained for the periods $\tau_{e11,o11}$, which are shown as solid lines in Fig. 6. On the same graph are shown experimental values for the period which were defined by the temperature difference between oscillation crests (i.e., between peak values of oscillation amplitude), and the corresponding temperature was taken to be halfway between peaks. The theoretical curves were fitted by using the previously determined value of a, and then e was determined by the best fit of the theory to the experimental data. We found typically $e \cong 0.36$ for our samples with an uncertainty due to the uncertainty in the core diameter ranging from

±0.01 for fiber C to ±0.03 for fiber B. In addition, the scatter of period values caused a random error in e of the order of ±2%.

One notices the excellent agreement between experiment and theory, which shows that the technique is applicable as an accurate way of measuring core ellipticity of liquid core fibers and should be comparable with the crossed polarizer technique.[14] Unlike the latter, however, the method presented here has the advantage of being nondestructive. Also it can be applied to measure the ellipticity along the fiber length over average intervals of the order of 10 cm by pulling the fiber through the furnace. Finally the crossed polarizer technique is restricted to measurements on the fundamental mode, while the method studied here can be performed on various modes, thereby providing a check as in the case of the diameter measurement.

VI. Conclusion

We have used the high-temperature dependence of the refractive index of the core of LCFs to vary v values over a large range and measured cutoff points of various low-order modes from transmitted and scattered radiation intensity. The experimental v_c values are in excellent agreement with the weakly guiding mode theory and have been used to calculate core radius to an accuracy of 5%. We have also shown for the first time the existence of two kinds of oscillations in the transmitted intensity caused by interference between modes. The theoretical interpretation allows identification of the modes involved and provides simultaneous measurement of core diameter and core ellipticity to very high precision. This nondestructive technique of geometrical characterization of hollow fibers is the first of the kind, easy to perform, and can probably be extended to solid core fibers. Presently we are extending the studies to solid core fibers.

We thank Hugo Fragnito and Alvin Kiel for many helpful discussions and Danilo Dini for technical help in designing the furnace.

This work was carried out in a project financed by Telebras S/A.

References

1. W. A. Gambling, D. N. Payne, and H. Matsumura, Electron. Lett. **9**, 412 (1973).
2. A. Papp and H. Harms, Appl. Opt. **16**, 1315 (1977).
3. K. Inada, in *Technical Digest, Seventh ECOC*, Copenhagen, 1981.
4. V. Ramaswamy, R. H. Stolen, M. D. Divino, and W. Pleibel, Appl. Opt. **18**, 4080 (1979).
5. A. Papp and H. Harms, Appl. Opt. **14**, 2406 (1975).
6. D. Gloge, Appl. Opt. **10**, 2252 (1971).
7. J. Stone, IEEE J. Quantum Electron. **QE-8**, 386 (1972).
8. E. Snitzer and H. Osterberg, J. Opt. Soc. Am. **51**, 499 (1961).
9. J. E. Midwinter and M. H. Reeve, Opto-electronics **6**, 411, (1974).
10. E. Bochove, unpublished work. We do not know the effects of refracting surfaces such as that of the liquid cell on the orthogonality of the transformed modes e'_n.
11. D. Marcuse, Bell Syst. Tech. J. **52**, 817 (1973).
12. A. W. Snyder and W. R. Young, J. Opt. Soc. Am. **68**, 297 (1978).
13. Y. Murakami, A. Kawana, and A. Tsuchiya, Appl. Opt. **18**, 1101 (1979).
14. S. R. Norman, D. N. Payne, M. J. Adams, and A. M. Smith, in *Technical Digest, Fifth ECOC*. Amsterdam, 1979.

Meetings Calendar *continued from page 2707*

1982
September

8–10 Optics 82 Conf., Edinburgh *Optical Group, Institute of Physics, 47 Belgrave Square, London SWIX 8QX, UK*

12–17 184th ACS Natl. Mtg., Kansas City, Mo. *A. T. Winstead, 1155 16th St. N.W., Wash., D.C. 20036*

19–23 4th Ann. Conf. Lasers in Graphics/Electronic Publishing in the 80's, Miami *R. Dunn, 1131 Beaumont Circle, Vista, Calif. 92083*

19–24 FACSS 9th Ann. Mtg., Phila. *A. Zander, Spectrametrics, Inc., 204 Andover St., Andover, Mass. 01810*

21–23 1st Int. Congr. on Applications of Lasers and Electro-Optics, Boston *H. Lee, LIA Bus. Off., 5151 Monroe St., Toledo, Ohio 43623*

21–24 VIII European Conf. on Optical Communication, Cannes *Secretariat General ECOC 1982, 11 rue de Hameline, 75783 Paris Cedex 16, France*

October

? Int. Symp. on the Measurement of Geometrical Quantities, Beijing, China *Secretariat, Chinese Society for Measurement, P.O. Box 1413, Beijing, China*

4–6 Technology for Space Astrophysics—The Next 30 Years Conf., Danbury *D. McCarthy, Mail Station 879, Perkin-Elmer Corp., 100 Wooster Hgts. Rd., Danbury, Conn. 06810*

4–8 Effective Engineering Management course, Boston *Cont. Ed. Inst., 10889 Wilshire Blvd., Suite 1030, Los Angeles, Calif. 90024*

4–8 IEEE's Industrial Applications Group, Electrostatics, Electrophotography and Electrostatic Precipitators, San Francisco *M. Hirsh, 28 Spier Ave., Rochester, N.Y. 14620*

5–8 Holographic Data Non-Destructive Testing Conf., Dubrovnik *D. Vukicevic, IFS—Inst. Phys., U. Zagreb, YU/41000 Zagreb, Bijenicka 45, Dubrovnik, Yugoslavia*

continued on page 2720